ELSEVIER

An approximate analytical solution to the Graetz problem with periodic inlet temperature

B. Fourcher and K. Mansouri
Laboratoire de Thermodynamique, Faculté, des Sciences et des Techniques de l'Université de Nantes, Nantes, France

Unsteady heat transfer for fully developed laminar flow with a parabolic velocity profile through a parallel-plate channel, subjected to sinusoidally varying inlet temperature is considered. A boundary condition which accounts for the effects of both external convection and wall thermal capacitance is considered. In this work, we develop a new approximate solution to this periodic Graetz problem, using a second-order Galerkin method. The present model neglects axial heat conduction along the wall but takes into account the transverse temperature gradient in the wall. The effects of transverse heat conduction in the wall and fluid-to-solid heat capacitance ratio on the behavior of the periodic responses are investigated. Comparisons are made with a finite difference solution.

Keywords: conjugate laminar forced convection; periodic inlet temperature; transient heat transfer in a parallel-plate channel

Introduction

Studies of sensible heat storage systems and regenerators require the dynamic response of an exchanger where the inlet temperature varies in time. The simplest, most expedient approach to this problem is the standard quasi-steady method which employs a constant surface heat transfer coefficient. Kardas (1966) investigated the heat transfer to flow in parallel-plate channels subjected to an inlet temperature varying with time. He presented an analytical solution of the unidirectional regenerator problem. He employed a quasi-steady model and Laplace transforms. Sparrow and De Farias (1968) investigated the transient laminar forced convection in a parallel-plate channel where the wall temperature was dynamically determined by a balance of the heat transfer rate and the energy storage. They also assumed that slug flow and the fluid inlet temperature varied sinusoidally. Kakaç and Yener (1973) obtained the exact solution to the transient energy equation for laminar slug flow in parallel plate channel with a sinusoidal variation of inlet temperature. They presented experimental results to predict the lowest eigenvalue for turbulent flow. Originally, Kakaç (1975) was the first to obtain an analytical solution, but only in the case of a constant wall temperature. Cotta et al. (1987) utilised the solution methodology suggested by Cotta and Ozisik (1986) to solve the conjugate laminar forced convection in parallel-plate ducts and circular tubes for slug flow with periodically varying inlet temperature. Guedes and Cotta (1991) examined the effects of axial conduction in the wall for laminar flow inside ducts, but the effects of transverse temperature gradients in the solid were neglected. The inlet temperature was assumed to vary periodically in time. Later, Guedes et al. (1994) extended their previous study to turbulent flow. Kakaç and Li (1994) compared the experimental results with theoretical studies under a general boundary condition which considered the external convection and the wall thermal capacitance. Recently, Mansouri and Fourcher (1995) analyzed the periodic forced convection with parabolic velocity profile in a parallel-plate channel. A second-order accurate explicit finite difference scheme was used in the numerical solution. The effects of the wall thickness and Biot number were investigated.

In this work, we developed a new approximate solution to solve laminar forced convection in parallel-plate ducts subjected to periodic variations of inlet temperature over time. We considered both parabolic flow and coupling with the walls. We begin by assuming a periodic solution relative to time and eliminate the axial dependance by Laplace transforms. Then the remaining fluid energy equation is solved by a second-order Galerkin method. Transverse conduction is allowed in the solid plate. To verify the pertinence of the proposed Galerkin method, we also solved this problem by using the technic of the numerical finite difference. The latter is validated by comparing with the exact analytical solution based on the hypothesis of the slug flow situation. The results are compared with the values given by Li and Kakaç (1991). They utilised a variation of the generalized integral transform technique, thus avoiding the complex eigenvalue problem and solving instead a coupled system of complex ordinary differential equations. The present methodology is presented to solve conjugate laminar forced convection inside the

Address reprint requests to Dr. B. Fourcher, Laboratoire de Thermodynamic, Faculté des Sciences et des Techniques de l'Université de Nantes, 2, Rue de la Houssinière 44072 Nantes cedex 03, France.

Received 29 March 1995; accepted 23 July 1996

Int. J. Heat and Fluid Flow 18:229–235, 1997

655 Avenue of the Americas, New York, NY 10010

0142-727X/97/$17.00
PII S0142-727X(96)00089-9

channel of a thick-walled heat exchanger and to evaluate its unsteady performance.

Formulation of the problem

We consider laminar forced convection inside parallel-plate channels subjected to periodic time variation in the inlet temperature. The geometry for the theoretical analysis is shown in Figure 1. Viscous dissipation and free convection are not taken into consideration, and physical properties are assumed to be constant. The duct wall external surface is subjected to convection with an environment at constant temperature T_∞, and heat conduction across the duct walls is taken into account. Axial conduction in the fluid is neglected. The effect of axial conduction in the fluid is indeed significant if Peclet number is less than ≈ 100 (Hsu 1968; Lin and Kuo 1988; Michelson and Villadsen 1974). The energy equation governing the diffusion in the z-axis and the convection in the x-axis can be written in a dimensionless form as:

Fluid region:

$$\partial^2\tilde{T}/\partial z^{+2} = U^+(z^+)\partial\tilde{T}/\partial x^+ + i\delta\tilde{T} \quad \text{for} \quad 0 < z^+ < 1,\ x^+ > 0 \tag{1a}$$

$$\tilde{T} = 1 \quad \text{at} \quad x^+ = 0 \tag{1b}$$

$$\partial\tilde{T}/\partial z^+ = 0 \quad \text{at} \quad z^+ = 0, \quad \text{for} \quad x^+ > 0 \tag{1c}$$

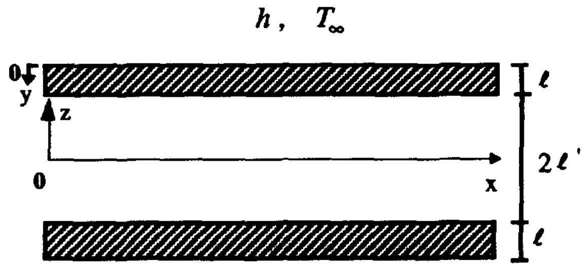

Figure 1 The geometry of the theoretical analysis

Solid region:

$$\partial^2\tilde{\theta}/\partial y^{+2} = 2i\beta_s^2\tilde{\theta} \quad \text{for} \quad 0 < y^+ < 1,\ x^+ > 0 \tag{2a}$$

$$\partial\tilde{\theta}/\partial y^+ = \mathrm{Bi}\,\tilde{\theta} \quad \text{for} \quad y^+ = 0,\ x^+ > 0 \tag{2b}$$

Solid–fluid interface:

$$\left\{\begin{array}{l}\tilde{T} = \tilde{\theta} \\ r\,\partial\tilde{\theta}/\partial y^+ = -\partial\tilde{T}/\partial z^+\end{array}\right. \quad \text{at} \quad y^+ = z^+ = 1 \text{ for } x^+ > 0 \tag{2c}$$

where the following dimensionless groups have been utilised: $x^+ = 4x/l'Pe$; $y^+ = y/l$; $z^+ = z/l'$; $\beta_s = l\sqrt{\pi/\tau\alpha_s}$; $\mathrm{Bi} = hl/\lambda_s$ $\delta = 2l'^2\pi/\tau\alpha_f$; $r = l'\lambda_s/l\lambda_f$; $T^+ = (T - T_\infty)/T_0$; $\theta^+ = (\theta -$

Notation

$[A]$	$N \times N$ matrix, defined by Equation 11a and b
a_{nk}	elements of coefficients matrix $[A]$
a^*	fluid-to-wall thermal capacitance ration $(= \rho_f C_f l'/\rho_s C_s l)$
A_n	complex coefficient, defined by Equation 15a
[B]	column vector of know values b_n
Bi	Biot number $(= hl/\lambda_s)$
$\overline{\mathrm{Bi}}$	modified Biot number $= r\mathrm{Bi}/(\mathrm{Bi} + 1)$
b_n	coefficient vector, defined by Equation 11c
[C]	column vector of unknow values C_n
C_s	wall specific heat
C_f	specific heat of the fluid at constant pressure
D_e	equivalent diameter $(= 4l')$
$\tilde{H}$	coefficient, defined by Equation 3c
h	convection heat transfer coefficient outside the wall
i	$\sqrt{-1}$
l	thickness of the wall
l'	half distance between parallel plates
$[M]$	square matrix for solving temperature field
$[P]$	column matrix of know values for solving temperature field
p	Laplace transform variable
Pe	Peclet number $(= \bar{u}D_e/\alpha_f)$
Q_n	complex coefficient, defined by Equation 15b
r	$(= l'\lambda_s/l\lambda_f)$
T	fluid temperature
T^+	dimensionless fluid temperature $= (T - T_\infty)/T_0$
T_0	amplitude of inlet temperature
T_∞	ambient temperature
t	time variable
$u(z)$	flow velocity
U^+	Dimensionless flow velocity $(= u(z)/\bar{u}$
$\bar{u}$	mean velocity
x, y, z	spatial coordinates

Greek

α	thermal diffusivity $(= \lambda/(\rho C_p)$
β_s	$(= l\sqrt{\pi/\tau\alpha_s})$
δ	dimensionless inlet frequency $(= 2l'^2\pi/\tau\alpha_f)$
ε	relative deviation
θ	solid temperature
θ^+	dimensionless solid temperature $= (\theta - T_\infty)/T_0$
λ	thermal conductivity
ξ	dimensional decay index defined in Equation 18
μ_n	complex root of equation $\det[A] = 0$
σ_n	complex eigenvalues of Equation 8
ρ	density
τ	period $(= 2\pi/\omega)$
φ	phase lag, Equation 17
χ	dimensionless temperature amplitude
ω	$(= 2\pi/\tau)$

Superscripts

b	bulk quantity
c	centerline value
f	fluid properties
N	number of terms in series
s	solid properties

Subscripts

$\sim$	time transformation defined by Equation 2d
$-$	Laplace transform with respect to the x^+ variable

$T_\infty)/T_0$; $U^+ = u(z)/\bar{u}$. Here, there is no need for an initial condition, because we are interested in the periodic solution of the problem. We seek a solution in the form:

$$T^+(x^+, z^+, t) = \tilde{T}(x^+, z^+)e^{i\omega t}$$

and (2d)

$$\theta^+(x^+, y^+, t) = \tilde{\theta}(x^+, y^+)e^{i\omega t}$$

where $i = \sqrt{-1}$.
The fully developed parabolic velocity profile $U^+(z^+)$ is

$$U^+(z^+) = 3/2(1 - z^{+2}).$$

The solution to Equation 2a is

$$\tilde{\theta} = A \sinh[\beta_s(1+i)y^+] + B \cosh[\beta_s(1+i)y^+] \quad (3a)$$

When we substitute Equation 3a into Equation 2b and 2c, we obtain the following equation:

$$\partial\tilde{T}(x^+, 1)/\partial z^+ + \tilde{H}\tilde{T}(x^+, 1) = 0 \quad (3b)$$

where

$$\tilde{H} = r(\text{Bi} + \tilde{\beta}_s \tanh\tilde{\beta}_s)/(1 + \text{Bi}\tanh\tilde{\beta}_s/\tilde{\beta}_s);\ \tilde{\beta}_s = (1+i)\beta_s \quad (3c)$$

Equation 3b is a boundary condition of the third kind with a complex exchange coefficient $\tilde{H}$, which includes the properties of the wall. If $\tilde{H}$ tends to infinity, Equation 3b gives a constant wall temperature boundary condition; if $\tilde{H}$ tends to zero, Equation 3b becomes an insulated boundary condition. Using the expression for $\tilde{\theta}$, Equation 3a, the following equation can be obtained:

$$\tilde{\theta}(y^+ = 1)/\tilde{\theta}(y^+ = 0) = \cosh\tilde{\beta}_s + \text{Bi}\sinh\tilde{\beta}_s/\tilde{\beta}_s \quad (4a)$$

For smaller values of β_s ($\tanh\beta_s \approx \beta_s$) and $\text{Bi} \ll 1$, the effect of heat conduction in the wall can be neglected. The coefficient $\tilde{H}$ becomes:

$$\tilde{H} = r\text{Bi} + i\delta/a^* \quad (4b)$$

where $a^* = (\rho C)_f l'/(\rho C)_s l$.
The parameter a^* represents the ratio of heat capacity of fluid to that of the wall. Li and Kakaç (1991) obtained for the convective boundary condition which considers the effect of wall thermal capacitance the following expression:

$$\tilde{H} = [r\text{Bi}/(\text{Bi}+1)] + i\delta/a^* \quad (4c)$$

For $\text{Bi} \ll 1$ (and $\beta_s \ll 1$), Equation 4b and 4c are equivalent, otherwise for $\text{Bi} \geq 1$ (and $\beta_s \ll 1$) Equation 3c becomes:

$$\tilde{H} = [r\text{Bi}/(\text{Bi}+1)] + [i\delta/a^*(\text{Bi}+1)] \quad (4d)$$

Approximate solution by Galerkin method

If we define the Laplace transform of the complex temperature as

$$\bar{\tilde{T}}(z^+, p) = \int_0^\infty \exp(-px^+)\tilde{T}(x^+, z^+)\,dx^+ \quad (5)$$

the transform of Equations 1a, 1c, and 3b, yields

$$L[\bar{\tilde{T}}] = d^2\bar{\tilde{T}}/dz^{+2} - 3/2(1 - z^{+2})(p\bar{\tilde{T}} - 1) - i\delta\bar{\tilde{T}} = 0 \quad (6a)$$

$$d\bar{\tilde{T}}/dz^+ = 0 \quad \text{at} \quad z^+ = 0 \quad (6b)$$

$$d\bar{\tilde{T}}/dz^+ = -\tilde{H}\bar{\tilde{T}} \quad \text{at} \quad z^+ = 1 \quad (6c)$$

To solve Equations 6, we employ the Galerkin method, where we approximate the solution by

$$\bar{\tilde{T}}_n(z^+, p) = \sum_1^N C_n(p)\cos(\sigma_n z^+) \quad (7)$$

where the function $\cos(\sigma_n z^+)$ satisfies the boundary conditions 6b and c. The eigenvalues σ_n are solutions of the transcendental equation

$$\sigma \tan\sigma = \tilde{H} \quad (8)$$

The unknown, complex coefficients $C_n(p)$ are given by employing orthogonality between the operator $L[\bar{\tilde{T}}]$ of Equation 6a and $\cos(\sigma_n z^+)$:

$$\int_0^1 L\left[\bar{\tilde{T}}_n(z^+, p)\right]\cos(\sigma_n z^+)\,dz^+ = 0 \quad \text{for} \quad n = 1 \quad \text{to} \quad N \quad (9)$$

Equation 9 can be expressed in matrix form as $[A][\mathbf{C}] = [\mathbf{B}]$ where $[A]$ is a square symmetric matrix with complex elements. The vector $[\mathbf{C}]$ is defined by

$$[C(p)] = \{C_1(p), C_2(p), \ldots, C_N(p)\} \quad (10)$$

and the elements (a_{nk}) of the matrix $[A]$ are given by

$$a_{nn} = (\sigma_n^2 + i\delta)\left(1 + \frac{\sin 2\sigma_n}{2\sigma_n}\right) + p + \frac{3p}{8}\left(\frac{\sin 2\sigma_n - 2\sigma_n\cos 2\sigma_n}{\sigma_n^3}\right) \quad (11a)$$

$$\underset{n \neq k}{a_{nk}} = a_{kn} = -6p\left[\frac{\cos\sigma_n\cos\sigma_k}{(\sigma_n^2 - \sigma_k^2)^2}(2\tilde{H}^2 + 2\tilde{H} + \sigma_n^2 + \sigma_k^2)\right] \quad (11b)$$

The vector $[\mathbf{B}]$ is defined by

$$b_n = \frac{6}{\sigma_n^3}(\sin\sigma_n - \sigma_n\cos\sigma_n) \qquad n = 1, 2, \ldots, N \quad (11c)$$

The Laplace transforms of the bulk temperature $\bar{\tilde{T}}_b(p)$ is defined by

$$\bar{\tilde{T}}_b(p) = 3/2\int_0^1 (1 - z^{+2})\bar{\tilde{T}}(z^+, p)\,dz^+ \quad (12)$$

then

$$\bar{\bar{T}}_b(p) = 1/2\sum_{1}^{N} b_n C_n(p) \tag{13}$$

After some algebraic manipulations we obtain

$$\bar{\bar{T}}_b(p) = \sum_{1}^{N} Q_n/(p+\mu_n) \tag{14}$$

where μ_n is a complex root of the characteristic Equation $\det[A]=0$ and Q_n is a complex quantity. The inverse transform of Equations 7 and 14 may be written respectively as:

$$\tilde{T}_c(x^+,0) = \sum_{1}^{N} A_n \exp(-\mu_n x^+) \tag{15a}$$

$$\tilde{T}_b(x^+) = \sum_{1}^{N} Q_n \exp(-\mu_n x^+) \tag{15b}$$

For $N=2$ it is possible to compute explicitly the constants A_n, Q_n, μ_n and obtain accurately the values of $\tilde{T}_c(x^+,0)$ and $\tilde{T}_b(x^+)$. It is convenient to define:

$$T_c(x^+,t) = \chi_c(x^+)\sin[\omega t - \varphi_c(x^+)] \tag{16a}$$

$$T_b(x^+,t) = \chi_b(x^+)\sin[\omega t - \varphi_b(x^+)] \tag{16b}$$

where

$$\chi_c(x^+) = |\tilde{T}_c(x^+)| \quad \text{and} \quad \varphi_c(x^+) = -\arg\tilde{T}_c(x^+) \tag{17a}$$

$$\chi_b(x^+) = |\tilde{T}_b(x^+)| \quad \text{and} \quad \varphi_b(x^+) = -\arg\tilde{T}_b(x^+) \tag{17b}$$

To compute the numerical results and the Galerkin methods, the dimensional decay index ξ is defined as:

$$\chi_c(x^+) = De^{-\xi x^+} \tag{18}$$

Validity of the method

The solution of Equations 1 and 3b was found by application of a finite-difference method. We used a fourth-order scheme in the z-direction and third-order in the x-direction. The system written in finite differences leads to the matrix equation

$$[M][T] = [P] \tag{19}$$

The complex Equation 19 has been numerically solved by using appropriate subroutines from IMSL library, 1987. The accuracy of the numerical scheme can be checked by using a slug flow velocity profile where an exact analytic solution has been developed by Acker and Fourcher (1981). In Table 1, the numerical and analytical decay indexes, respectively ξ(num) and ξ(anal), have been listed and compared. The maximum relative deviation is less than 1% for different a^*. Excellent agreement is found for parabolic flow between the numerical results and the Galerkin methods.

Results and discussion

Based on the preceding analysis, we now present some typical results for the dimensionless centerline and bulk temperature.

Table 1 Comparison of decay index values (ξ) obtained from the Galerkin methods and numerical solution (Bi=0.0 and δ=0.1)

a^*	ξ (num.)	ξ (anal.)	ε, percent
5. 10^{-5}	1.88482	1.88398	0.045
8.5 10^{-3}	1.85130	1.85138	0.004
8.5 10^{-2}	0.52042	0.52084	0.081
0.1	0.42310	0.42130	0.425

Numerical values for the parameters a^*, and $\overline{\mathrm{Bi}}$, and δ followed those in Li and Kakaç (1991). The effects of heat conduction in the wall and thermal capacitance on the temperature amplitudes and phase lags were then investigated, with particular emphasis on the transverse wall diffusion, because this aspect was not considered in previous works available.

Figures 2 and 3 illustrate the effects of fluid-to-wall thermal capacitance ratio on the bulk temperature amplitudes and the phase lags along the duct for Bi = 8.5 10^{-4} and 8.5 10^{-3} corresponding, respectively, to $\overline{\mathrm{Bi}}$ = 10 and 100 at δ = 0.1. It can be seen that for large values of wall thermal capacitance (small $a^* \approx 0.01$), the storage of heat in the wall will substantially affect the dimensionless temperature amplitude along the duct, especially for values of Biot number less than 8.5 10^{-4} (see Figure 2). The effect will be more significant for the phase lags. From these two figures, it is clear that the differences among the temperature amplitudes and the phase lags along the duct for different a^* at small values of Bi($<8.5\ 10^{-4}$) are substantial, while those differences for large values of Bi (i.e., 8.5 10^{-3}) are very small; i.e., all the curves for different a^* are very close to each other (see Figure 3). When Bi is relatively large, the heat transfer by external convection is predominant, and the effect of a^* on the temperature amplitude along the duct is then small (for Bi = 8.5 10^{-3}).

Figure 4 shows the amplitudes of the centerline temperature along the channel for different β_s by fixing a^* = 8.5 10^{-3} and δ = 0.1. This particular value of a^* corresponding to the practical

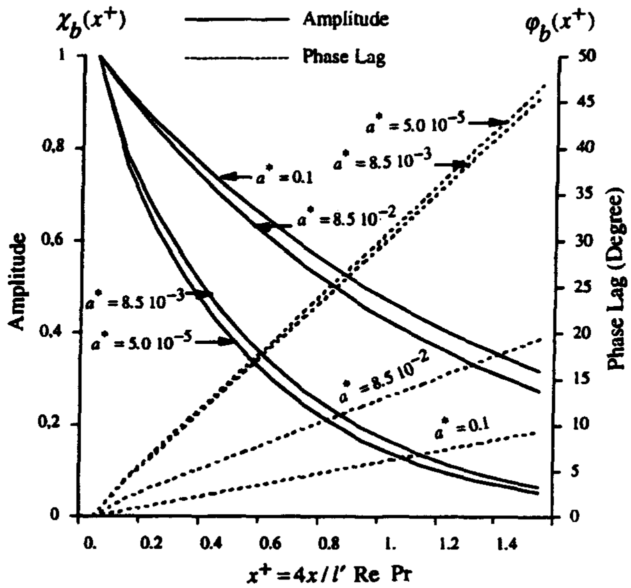

Figure 2 Amplitudes and phase lags of dimensionless bulk temperature along the duct for various values of fluid-to-wall thermal capacitance ratio (Bi=8.5 10^{-4}; δ=0.1)

Table 2 The first two coefficients and eigenvalues for bulk temperature of considering the effects of wall conduction; at Bi = 0.0 and δ = 0.1

n	Q_n	μ_n	σ_n	a^*
1	0.90942E+0 − 5.45678E − 4i	0.18840E+1+0.77778E − 1i	1.57077E+0+8.08840E − 4i	5. 10⁻⁵
2	6.97397E − 2+1.41805E − 4i	0.22554E+2+0.11006E+0i	4.71231E+0+2.42655E − 3i	
1	0.91608E+0 − 2.71150E − 2i	0.18514E+1+0.34697E+0i	1.55922E+0+1.33295E − 1i	8.5 10⁻³
2	6.48534E − 2+9.02926E − 3i	0.21999E+2+1.58021E+0i	4.66997E+0+4.19288E − 1i	
1	1.01478E+0 − 1.95309E − 2i	0.52113E+0+0.96569E+0i	8.64887E − 1+5.85492E − 1i	8.5 10⁻²
2	−1.61903E − 2+1.91835E − 2i	0.14282E+2+3.91168E+0i	3.18842E+0+3.68781E − 1i	
1	1.01292E+0 − 1.41387E − 2i	0.42159E+0+0.90484E+0i	0.80050E+0+5.69880E − 1i	0.1
2	−1.23032E − 2+1.40298E − 2i	0.14108E+2+3.36126E+0i	3.17666E+0+3.21920E − 1i	
1	1.00003E+0 − 5.14392E − 7i	4.09960E − 4+1.09997E − 1i	7.08401E − 2+7.05808E − 2i	10
2	−2.80479E − 5+5.15163E − 7i	0.13351E+2+1.92757E − 1i	3.14160E+0+3.18311E − 3i	
1	1.00001E+0+9.46708E − 7i	2.05260E − 4+1.00999E − 1i	2.23681E − 2+2.23432E − 2i	100
2	−1.35821E − 5 − 9.46806E − 7i	0.13351E+2+1.63524E − 1i	3.14159E+0+3.18310E − 4i	

case (the fluid is a gas and the wall is a styrofoam) considered by Kakaç and Li (1994). The curves for different β_s represent the effects of the transverse temperature gradients in the solid. For decreasing β_s, which represents a decrease in the wall heat conduction, the amplitude decays faster along the channel. From Figure 4, the phase lags of the dimensionless centerline temperature distributions are presented for the same numerical values of a^* and δ. For decreasing values of β_s, the delay becomes smaller (decreasing phase lags). It can be seen that for large values of β_s (i.e., 5.0), the effects of the transverse temperature gradients in the wall are more pronounced.

Based on the cases studied here, the phase lag varies linearly with the dimensionless axial distance x^+ along the channel. Generally, for regions sufficiently away from the inlet, only the principal mode (μ_1) of the exponential series is dominant. Therefore, the temperature amplitude decays exponentially along the distance from the inlet except at the locations very close to the inlet. The important results of the theoretical analysis are also given in tabular form. In Table 2, the first two coefficients Q_n and eigenvalues (μ_n and σ_n) are listed for different a^* and Bi = 0. These values can be used in Equations 15a and b to calculate numerical values of centerline and bulk temperature respectively.

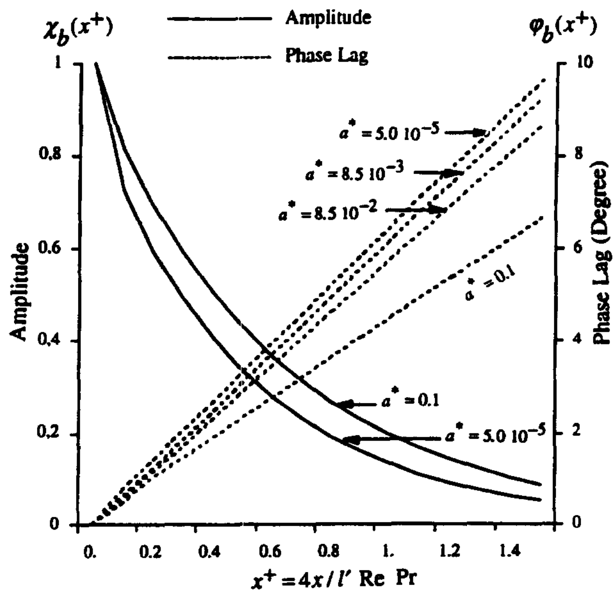

Figure 3 Amplitudes and phase lags of dimensionless bulk temperature along the duct for various values of fluid-to-wall thermal capacitance ratio (Bi = 8.5 10^{-3}; δ = 0.1)

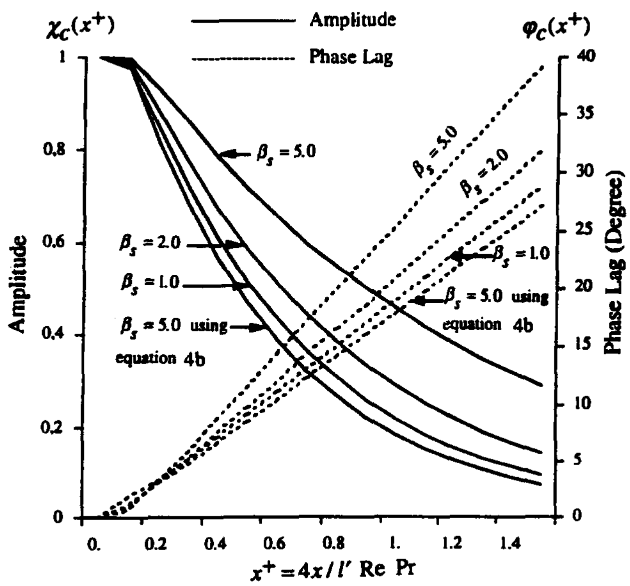

Figure 4 Amplitudes and phase lags of dimensionless temperature along the centerline of the duct for different values of β_s (a^* = 8.5 10^{-3}, δ = 0.1 and Bi = 0.0)

Table 3 Comparison of the eigenvalues and coefficients with the values given by Li and Kakaç for centerline temperature using Equation 4c; at Bi=0.0 and δ=0.1

n	A_n (present study)	A_n (Li and Kakaç)	μ_n (present study)	μ_n (Li and Kakaç)	a^*
1	0.12020E+1+0.66345E−3i	0.12072E+1+0.82011E−3i	0.18840E+1+0.77778E−1i	0.20117E+1+0.72862E−1i	$5.\ 10^{-5}$
2	−0.29824E+0−0.32141E−3i	−0.31090E+0−0.95008E−3i	0.22554E+2+0.11006E+0i	0.22407E+2+0.10293E+0i	
1	0.12032E+1+0.15604E−1i	0.12093E+1+0.14771E−1i	0.18514E+1+0.34697E+0i	0.19728E+1+0.37485E+0i	$8.5\ 10^{-3}$
2	−0.29020E+0−0.32970E−1i	−0.31598E+0−0.27488E−1i	0.21999E+2+0.15802E+1i	0.22009E+2+0.24615E+1i	
1	0.10689E+0+0.11381E+0i	0.1064E+1+0.11674E+0i	0.42159E+0+0.90484E+0i	0.40422E+0+0.92886E+0i	0.1
2	−0.71301E−1−0.13277E+0i	−0.72035E−1−0.15280E+0i	0.14108E+2+0.33613E+1i	0.12772E+2+0.28317E+1i	

$a^*=8.5\ 10^{-3}$ and $\delta=0.1$

n	A_n (present study)	A_n (Li and Kakaç)	μ_n (present study)	μ_n (Li and Kakaç)	$\overline{Bi}$
1	0.12030E+1+0.15726E−1i	0.12083E+1+0.14892E−1i	0.18491E+1+0.34612E+0i	0.19703E+1+0.37647E+0i	0.1
2	−0.29051E+0−0.36584E−1i	−0.31556E+0−0.27771E−1i	0.22003E+2+0.16081E+1i	0.21986E+2+0.24723E+1i	
1	0.12017E+1+0.16591E−1i	0.12073E+1+0.16102E−1i	0.18302E+1+0.33682E+0i	0.19432E+1+0.38806E+0i	1.0
2	−0.28972E+0−0.69402E−1i	−0.31352E+0−0.30440E−1i	0.21955E+2+0.187918E+1i	0.21762E+2+0.25467E+1i	

Space limitations preclude the complete tabulation for all cases considered here. Table 3 shows the comparison between the eigenvalues and coefficients, as calculated by solving the present model, and those calculated from the generalized integral transform technique by Li and Kakaç (1991). The discrepancy between the two methods is estimated at 6% for the principal mode μ_1.

Concluding remarks

The present model using a Galerkin method succeeds in predicting the temperature distribution inside a parallel-plate channel with periodically varying inlet temperature and convective boundary conditions, including the effects of transverse diffusion in the wall. The numerical scheme results and Galerkin method analyses are in excellent agreement. The results obtained in the present study can be briefly summarized as follows:

(1) For regions sufficiently away from the inlet only the first term of the series is necessary. Therefore, the fluid temperature amplitude decays exponentially with distance along the duct and the phase lag varies linearly.
(2) The effects of the heat capacitance ratio a^* are more pronounced at small Biot number.
(3) At a fixed frequency $\delta = 0.1$ considered here, the effects of the wall transverse conduction are more pronounced at large values of β_s.
(4) The present method is compared with the Li and Kakaç (1991) solution for the same boundary condition at the interface. The discrepancy is about 6% for the principal mode μ_1.

References

Acker, M. T. and Fourcher, B. 1981. Analyse en régime thermique périodique du couplage conduction–convection entre un fluide en écoulement laminaire et une paroi de stockage. *Int. J. Heat Mass Transfer*, **24**, 1201–1210

Cotta, R. M., Mikhailov, M. D., and Ozisik, M. N. 1987. Transient conjugated forced convection in ducts with periodically varying inlet temperature. *Int. J. Heat Mass Transfer*, **30**, 2073–2082

Cotta, R. M. and Ozisik, M. N. 1986. Laminar forced convection inside ducts with periodic variation of inlet temperature. *Int. J. Heat Mass Transfer*, **29**, 1495–1501

Guedes, R. O. C. and Cotta, R. M. 1991. Periodic laminar forced convection within ducts including wall heat conduction effects. *Int. J. Eng. Sci.*, **29**, 535–547

Guedes, R. O. C., Ozisik, M. N. and Cotta, R. M. 1994. Conjugated periodic turbulent forced convection in a parallel plate channel. *J. Heat Transfer*, **116**, 40–46

Hsu, C. J. 1968. Exact solution to entry-region laminar heat transfer with axial conduction and the boundary condition of the third kind. *Chem. Eng. Sci.*, **23**, 457–468

Kakaç, S. and Yener, Y. 1973. Exact solution of the transient forced convection energy equation for timewise variation of inlet temperature. *Int. J. Heat Mass Transfer*, **16**, 2205–2214

Kakaç, S. 1975. A general analytical solution to the equation of transient forced convection with fully developed flow. *Int. J. Heat Mass Transfer*, **18**, 1449

Kakaç, S. and Li, W. 1994. Unsteady turbulent forced convection in a parallel plate channel with timewise variation of inlet temperature. *Int. J. Heat Mass Transfer*, **37**, 447–456

Kardas, A. 1966. On a problem in the theory of the unidirectional regenerator. *Int. J. Heat Mass Transfer*, **9**, 567–579

Li, W. and Kakaç, S. 1991. Unsteady thermal entrance heat transfer in laminar flow with a periodic variation of inlet temperature. *Int. J. Heat Transfer*, **34**, 2581–2592

Lin, T. F. and Kuo, J. C. 1988. Transient conjugated heat transfer in fully developed laminar pipe flows. *Int. J. Heat Mass Transfer*, **31**, 1093–1102

Mansouri, K. and Fourcher, B. 1995. Réponse à un signal thermique sinucoïdal dans le cas d'un écoulement laminaire à plan directeur. *Int. Comm. Heat and Mass Transfer*, **22**, 305–315

Michelsen, M. L. and Villadsen, J. 1974. The Graetz problem with axial heat conduction. *Int. J. Heat Mass Transfer*, **17**, 1391–1402

Sparrow, E. M. and De Farias, F. N. 1968. Unsteady heat transfer in ducts with time-varying inlet temperature and participating walls. *Int. J. Heat Mass Transfer*, **11**, 837–853